2008

Vapor Shear Effects on Falling-Film Mode Transitions Between Horizontal Tubes

Binglu Ruan
Xi'an Jiaotong University

Anthony M. Jacobi
University of Illinois at Urbana-Champaign

Liansheng Li
Xi'an Jiaotong University

Vapor Shear Effects on Falling-film Mode Transitions between Horizontal Tubes

Binglu RUAN [1,2], Anthony M JACOBI [2*], Liansheng LI [1]

1. National Engineering and Research Center of Fluid Machinery and Compressor, Xi'an Jiaotong University, Xi'an, PR of China, 710049 (ruanbl@uiuc.edu, lils@mail.xjtu.edu.cn)
2. Mechanical Science and Engineering, University of Illinois, Urbana, IL, 61801(a-jacobi@uiuc.edu)
* Corresponding Author

ABSTRACT

A liquid falling between horizontal tubes can take the form of droplets, jets, or a continuous sheet mode, depending on the flow rate. The so-called falling-film flow regime is important to heat and mass transfer, and to maintaining wetted-surface conditions in a falling-film tube bundle, and the performance of such tube bundles is important in many air-conditioning systems. In this paper, we review prior work on falling film mode transitions between horizontal tubes and investigate vapor shear effects on the mode transitions. It is shown that vapor shear effects on mode transitions depend on liquid properties. Mode transition hysteresis is reduced by an increasing gas flow velocity. It is also found that the liquid feeding length can have an impact on falling-film mode transitions.

1. INTRODUCTION

Falling-film horizontal tube heat exchangers have been widely used in chemical, refrigeration, petroleum refining, desalination and food industries as evaporators, condensers and absorbers. These heat exchangers provide higher heat transfer coefficients and operate with smaller liquid inventories than flooded heat exchangers. They also mitigate fouling, non-condensable-gas effects and some other heat exchanger problems.

When a liquid flows from a distributor onto horizontal tubes, with an increasing flow rate, three basic modes will be observed (see Mitrovic, 1986): droplet, jet, and a continuous sheet. These modes may play an important role in the heat and mass transfer processes. Hu and Jacobi (1996a,1996b) suggested a slightly more detailed flow pattern classification for the mode transitions with a quiescent vapor, as shown in Fig. 1 and provided the first generalized flow pattern map for predicting the flow modes, also shown in Fig. 1.

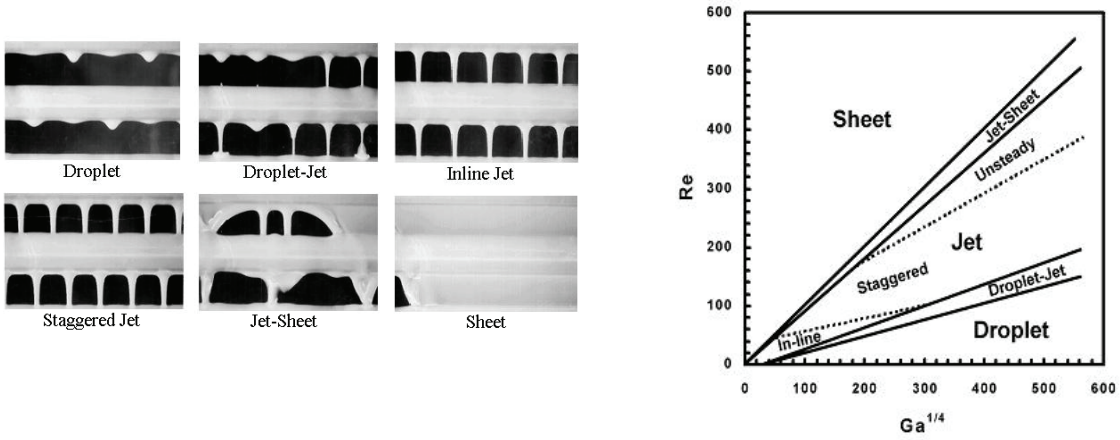

Figure 1: The falling-film modes between horizontal tubes and flow regime map of Hu and Jacobi, 1996a, 1996b.

Thome (1999) provided a comprehensive review of the state of the art for falling-film evaporation, and recently Ribatski and Jacobi (2005) presented a critical review of falling-film horizontal-tube evaporators for the purpose of

identifying opportunities for air-conditioning and refrigeration applications and areas where further research is needed. The most relevant papers, as discussed in those reviews, are outlined below.

Armbruster and Mitrovic (1994) described experiments using water and isopropyl alcohol and indicated that mode transitions among the droplet, jet, and sheet modes could be expressed in the following general form: $\mathrm{Re} = \mathrm{AGa}^{1/4}$,where A is an empirical constant. They also found the transitions to depend solely on the liquid flow rate. Equations for mode transitions were given and can be interpreted as:

$$\text{Droplet} \Leftrightarrow \text{Droplet-Jet:} \quad Re = 0.2Ga^{1/4} \tag{1}$$

$$\text{Droplet-Jet} \Leftrightarrow \text{Jet:} \quad Re = 0.26\ Ga^{1/4} \tag{2}$$

$$\text{Jet} \Leftrightarrow \text{Jet-Sheet:} \quad Re = 0.94\ Ga^{1/4} \tag{3}$$

$$\text{Jet-Sheet} \Leftrightarrow \text{Sheet:} \quad Re = 1.14\ Ga^{1/4} \tag{4}$$

Based on more than 1000 experimental observations, Hu and Jacobi (1996a, 1996b) studied mode transitions with water, ethylene glycol, hydraulic oil, a water/ethylene glycol mixture and alcohol. They found the mode transitions were relatively independent of geometric effect (tube diameter and spacing). In a simplified map neglecting hysteresis, they found the mode transitions were given by following equations:

$$\text{Droplet} \Leftrightarrow \text{Droplet-Jet:} \quad Re = 0.074\ Ga^{0.302} \tag{5}$$

$$\text{Droplet-Jet} \Leftrightarrow \text{Jet:} \quad Re = 0.096\ Ga^{0.301} \tag{6}$$

$$\text{Jet} \Leftrightarrow \text{Jet-Sheet:} \quad Re = 1.414\ Ga^{0.233} \tag{7}$$

$$\text{Jet-Sheet} \Leftrightarrow \text{Sheet:} \quad Re = 1.448\ Ga^{0.236} \tag{8}$$

Roques *et al.* (2002, 2003) provided equations for falling-film mode transitions on the basis of experiments with water, ethylene glycol and a water/ethylene glycol mixture:

$$\text{Droplet} \Rightarrow \text{Droplet-Jet:} \quad Re = 0.0417\ Ga^{0.3278} \tag{9}$$

$$\text{Droplet-Jet} \Rightarrow \text{Jet:} \quad Re = 0.0683\ Ga^{0.3204} \tag{10}$$

$$\text{Jet} \Rightarrow \text{Jet-Sheet:} \quad Re = 0.8553\ Ga^{0.2483} \tag{11}$$

$$\text{Jet-Sheet} \Rightarrow \text{Sheet:} \quad Re = 1.068\ Ga^{0.2563} \tag{12}$$

Mitrovic (2005) compared these correlations from the literature and found that they agreed well with each other. However, this prior work and the transition equations provided above are limited to quiescent surroundings, but significant vapor shear is present in many falling-film applications, and this vapor shear could impact the mode transitions or even destroy the modes and lead to local dry out. Limited studies of vapor shear effects on the mode transitions have been reported. In 2002, Wei and Jacobi (2002) conducted experiments with a countercurrent gas flow using ethylene glycol. Based on limited data, they suggested a new classification of modes and developed a new flow regime map, as shown in Fig.2. They found that as *We* increased, the hysteretic effect at transition decreased. Unfortunately, in addition to the limited data (ethylene glycol only) their classification scheme was overly complicated.. More data including different fluid properties and geometries will be provided in this paper.

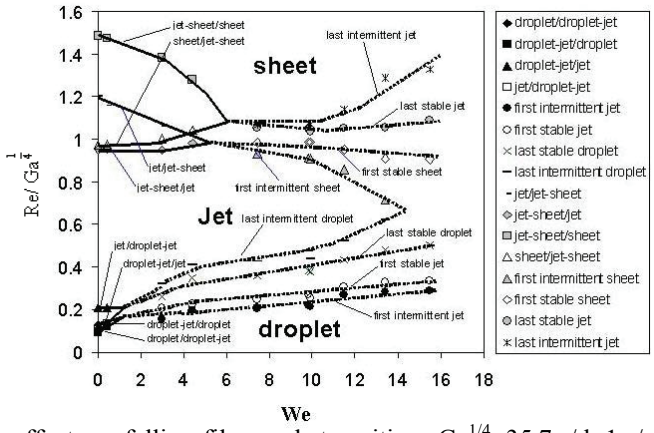

Figure 2: Vapor shear effects on falling-film mode transitions,$Ga^{1/4}$=35.7,s/d=1,s/a=9.3 (Wei and Jacobi, 2002)

2. EXPERIMENTAL APPROACH

2.1 Experiment Apparatus

A schematic of the experimental apparatus is given in Fig. 3. The apparatus consisted of a closed-circuit liquid circulation loop and an open-loop wind tunnel, intersecting at the test section. The liquid circulation loop consisted of a reservoir, a liquid pump, a filter, a flowmeter, two needle valves and a liquid collector. The speed-adjustable pump delivered the test liquid from the reservoir through a filter, a flowmeter and two needle valves to the test section. In order to get a uniform liquid distribution on the test tubes, the flow was divided into two parts and fed into the distributer from opposite directions. The liquid feeding system design is shown in Fig. 4. The primary distribution was completed by a PVC tube with 61 holes, 3 mm in diameter, 5 mm apart (center to center) on the bottom. The secondary distribution was achieved by a plexiglass box with 60 holes, 1 mm in diameter, 5 mm apart (center to center) on the bottom. The positions of the secondary distribution holes were carefully adjusted to be aligned with the primary distribution tube. When incoming flow went into the PVC tube from opposite directions, it passed the holes on the bottom of the tube into the plexiglass box, and then it built a liquid level or even filled up the box if the flow rate was large. This approach helped to ensure that a uniform axial liquid distribution was achieved. The gap between the bottom of the feeding tube and the top of the first test tubes was 1mm. After distribution by the feeding system, the liquid flowed around the first test tube, then fell to the second tube, then the third, and then fell to the liquid collector and eventually returned to a reservoir.

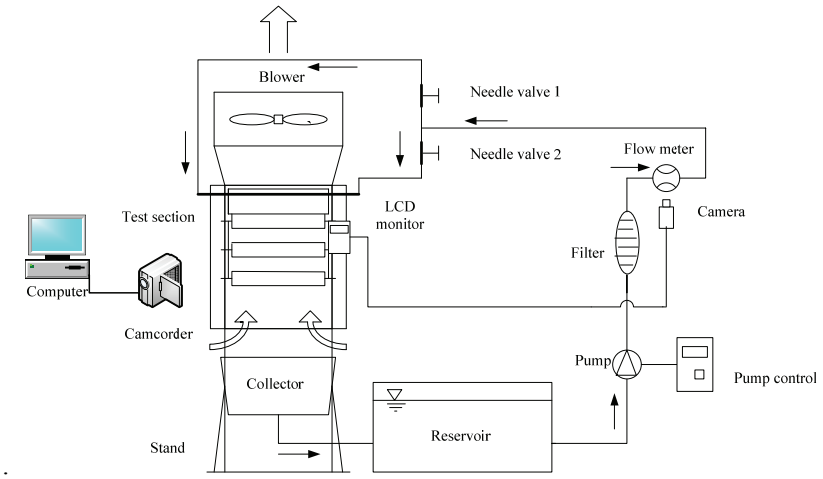

Figure 3: Schematic of the experimental apparatus

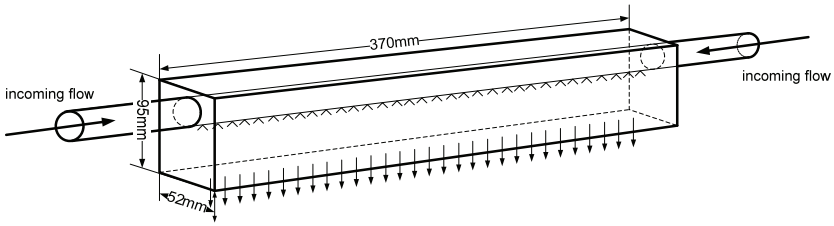

Figure 4: Feeding system design

The purpose of the wind tunnel was to impose interfacial vapor shear (and pressure) on the liquid film as it fell from tube to tube, to mimic conditions that can occur in application. The wind tunnel consisted of a blower and the test section. The test section, with a cross section of 250mm by 405mm was made of Plexiglas in order to obtain a better view of the test section. The sides of the test section supported the feeding system and the test tubes and allowed easy adjustment of the arrangement of test tubes. The wind tunnel could provide an air velocity up to 15 m/s and the approach velocity profiles were flat to with in 5 percent at the maximum blower speed.

2.2 Instrumentation

The liquid mass flow rate was measured using a Coriolis-effect flowmeter (± 0.1%). The fluid density and temperature were also measured using this instrument. Surface tension and viscosity of the test fluid were taken from the literature, based on the measured temperatures. The air flow profiles in the test section and turbulence intensity were recorded by a VELOCICALC air velocity meter, with an accuracy of 2.5%. Air density was inferred from laboratory temperature, humidity and pressure. An LCD monitor was placed in front of the test section to record the instrument displays, while a camcorder was simultaneously used to record flow patterns and mode transitions. The video images acquired by the camcorder were analyzed using a computer and standard image-processing software.

2.3 Test Procedure and Scope

Prior to a test, all of the brass tubes used in the experiment were polished with the emery cloth 320/P400. Tubes were placed at desired spacing in the test section. The tubes were carefully leveled by circulating liquid to obtain a jet mode and adjusting the tubes until the jets fell from fixed sites, without shifting in either direction. Tubes were fully wetted by circulating the test liquid in the system for 2~3 hours. The programmed pump control was set to run the pump from high frequency to low frequency or from low frequency to high frequency to achieve a decreasing or increasing flow supply to the test section.

During the experiments, the liquid mass flow rate, density, temperature, laboratory temperature, laboratory pressure and humidity were measured. The programmed pump provided the liquid flow and the data were recorded using a computer. In order to study hysteretic mode transitions, both slowly increasing and decreasing liquid flow rates were used, and five cycles were used (decreasing/increasing five times). Following tests in quiescent surroundings, the blower was used to supply a countercurrent air flow at several fixed velocities. Other than use of the blower, the same experimental procedures were adopted to study vapor shear effects on falling-film mode transitions.

Experiments were conducted using water and ethylene glycol with and without a countercurrent gas flow. For a falling film surrounded by a gas flow, the falling-film modes could depend on nine physical parameters, the experiment scope of which are provided in Table 1. Five dimensionless parameters can be defined to characterize the mode transitions using dimensional analysis. The test ranges and estimated experimental uncertainties of these groups are given in Table 2.

Table 1: Experimental range of the relevant physical variable

Physical Parameter	Experimental Range	Units
Mass flow rate per unit length, Γ	up to 0.3	kg/m·s
Liquid dynamic viscosity, μ	$1.0(10^{-3})$ to $2.0(10^{-2})$	N·s/m^2
Mass density of the liquid, ρ	998.8 to 1115	kg/m^3
Gas/liquid surface tension, σ	$4.8(10^{-2})$ to $7.3(10^{-2})$	N/m
Tube diameter, d	$25.4(10^{-3})$	m
Tube spacing, s	$11(10^{-3})$, $24(10^{-3})$, $45(10^{-3})$	m
Liquid feeding length, L	0.05~0.295	m
Gravitational acceleration, g	fixed at 9.8	m/s^2
Gas velocity U_g	Up to 6	m/s
Gas density ρ_g	1.2	kg/m^3

Table 2: Relevant dimensionless parameters, the experimental range and typical uncertainty

Dimensionless Parameter	Experimental Range	Uncertainty
$Re=2\,\Gamma/\mu$	up to 600	1%
$Ga=\rho\,\sigma^3/g\,\mu^4$	$7.4(10^4)$ to $4.7(10^{10})$	4%
s/d	0.433,0.945,1.77	1%
s/a	4.03 to 16.5	1%
$We=\rho_g\,U_g^2 d/\,\sigma$	up to 21.5	4%

3. RESULTS

3.1 Mode Classification

In quiescent surroundings, Hu and Jacobi (1996a, 1996b) defined five modes with four mode transitions (unsteady jets, staggered jets, and inline jets were classified into one jet mode). However, with an increasing *We*, the falling-film flow becomes unsteady, and mode classification becomes more difficult. Wei and Jacobi (2002) provided 16 mode transitions for falling-film behavior with a countercurrent gas flow, the utility of such detailed classification is dubious. In this paper, a simple mode classification is adopted, as given in Table 3—it is suitable for both steady flows and unsteady flows.

Table 3: A simple mode classification

Mode Transition (Abbreviation)		Definition/Characterization
Decreasing Flow Rate	Sheet $\Rightarrow$ Sheet-Jet (S-SJ)	The sheet first breaks into small sheets or sheets and jets.
	Sheet-Jet $\Rightarrow$ Jet (SJ-J)	The last small sheet breaks into jets.
	Jet $\Rightarrow$ Droplet-Jet (J-DJ)	The first droplet site appears among jets.
	Droplet-Jet $\Rightarrow$ Droplet (DJ-D)	The last jet becomes droplets.
Increasing Flow Rate	Droplet $\Rightarrow$ Droplet-Jet (D-DJ)	A jet first appears among droplets sites.
	Droplet-Jet $\Rightarrow$ Jet (DJ-J)	The last droplet site becomes a jet.
	Jet $\Rightarrow$ Jet-Sheet (J-JS)	The first small sheet appears among jets.
	Jet-Sheet $\Rightarrow$ Sheet (JS-S)	An intact sheet first appears.

3.2 Liquid Feeding Length Effects on Falling-film Mode Transitions

As part of our preliminary efforts to obtain a flat velocity profile in the gas flow, different liquid feeding lengths, *L*, were used in some experiments. While these results are not the main contribution of this work, they may be of interest to others working in the area. The data are presented as transitional $Re/Ga^{1/4}$ plotted against *L* (at fixed *s/d*) in Fig. 5. Clearly, the effect of *L* depends on *Ga*: for a fluid with $Ga^{1/4}\approx429$, the mode transitions show little dependence on *L*, but at $Ga^{1/4}\approx17$ the value of $Re/Ga^{1/4}$ for a transition from jet mode to jet-sheet mode drops sharply from 1.7 to 1.25 as *L* increases from 0.1m to 0.25 m. Because these effects are manifest in the J-JS and SJ-J transitions at low Ga, they might be due to edge effects that are important to sheet break-up and formation under steady-flow conditions. At $Ga^{1/4}\approx17$ these transitions occur between very stable, steady flows, but at $Ga^{1/4}\approx429$ these flow regimes occur with some unsteadiness. The data also suggest that transition hysteresis for the $Ga^{1/4}\approx429$ fluid is reduced at larger *L*. Wei and Jacobi (2002) indicated that higher *Ga* fluids exhibited unsteadiness and due to the unsteadiness in the flow, hysteresis was less evident in the mode transitions. Reducing *L* seems to have a similar effect, reducing the unsteadiness, even at higher *Ga*.

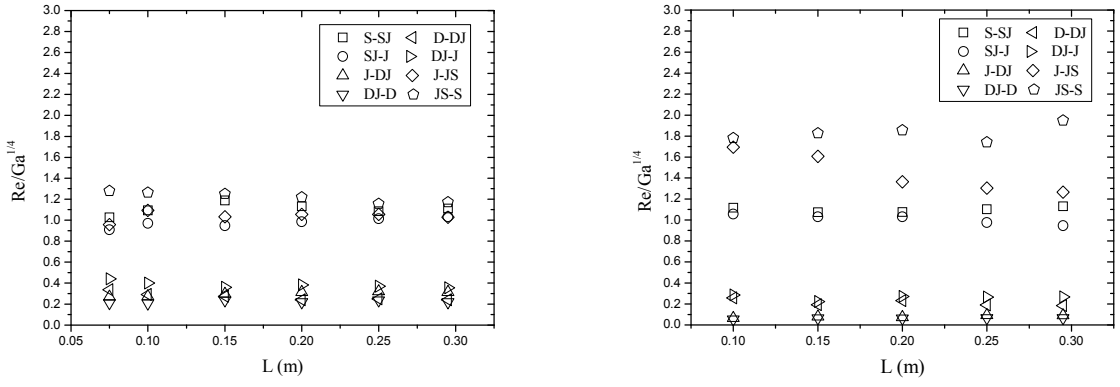

Figure 5: Liquid feeding length effects on falling-film mode transitions. (a) is for water, $Ga^{1/4}\approx429$; (b) is for ethylene glycol, $Ga^{1/4}\approx17$, and s/d=0.95. These data were obtained with a quiescent gas.

3.3 Mode Transitions with a Countercurrent Gas Flow

Data obtained under quiescent conditions were found to be in excellent agreement with the literature (see Eqs. 1-12), and experiments with a vapor flow were undertaken for *We,* up to 21.5 (U_g=5.8m/s). With an increasing *We*, the falling-film flow became more and more unsteady, and when the vapor velocity was larger than about 3.5m/s, stable, steady modes were not usually present. Based on the results presented above, a feeding length of *L*= 0.1m was adopted during the experiments with water ($Ga^{1/4}$≈465) . Transitional $Re/Ga^{1/4}$ are plotted against *We* in Fig. 6. It is shown that transitions between the droplet and droplet-jet, droplet-jet and jet, and jet-sheet and sheet required a higher *Re* for increasing *We,* due to unsteadiness caused by the air flow. However, transitions between jet and jet-sheet required a lower *Re* when *We* is increased, which might be due to increased jet diameters and film thicknesses when the countercurrent vapor flow was imposed. The data reported by Wei and Jacobi (2002) display the same trends with an increasing *We*, but they provided no explanation for this behavior.

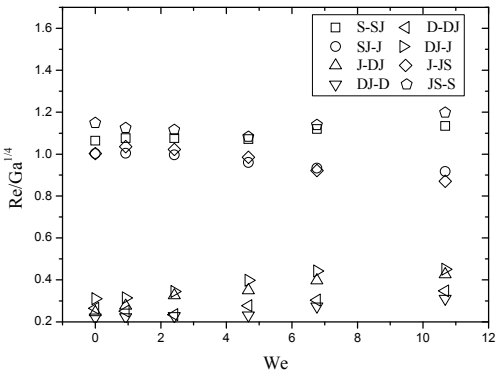

Figure 6: Vapor-shear effects on falling-film mode transitions, $Ga^{1/4}$=465 (Water), s/d=0.95,s/a=8.82,L=0.1m.

The dependence of the data on geometry can be ascertained by examining the results shown in Fig. 7, where transition data are provided for varying s/d. With an increasing *We*, very little dependence on s/d was reflected over range of these experiments. Of course, over a wider range a geometric effect might be important; more data are needed to further explore geometric effects on falling-film mode transitions with a countercurrent gas flow imposed.

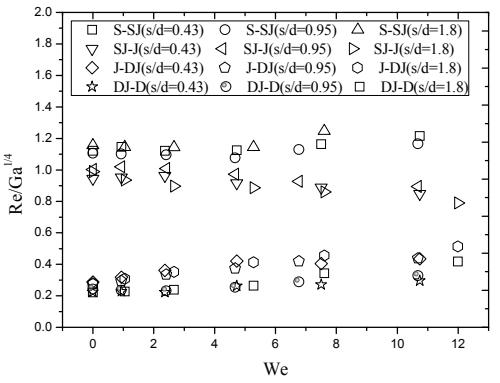

Figure 7: Vapor-shear effects on falling-film mode transitions with different geometry factor s/d, without considering hysteresis effect, $Ga^{1/4}$≈450 (Water).

Because the liquid feeding length has an impact on mode transitions for lower *Ga* liquids, vapor-shear experiments using ethylene glycol ($Ga^{1/4}$≈17) were conducted at two different liquid feeding lengths, *L*=0.1m and *L*=0.295m. The results are shown in Fig. 8, and by comparing the *L*=0.1m case to the *L*=0.295m case at *We=0*, it is clear that hysteresis is reduced with an increased *L* (consistent with §3.2). However, with an increasing *We* mode transitions at both *L* showed the same trends: For a decreasing liquid feeding rate, all transitions occur at a higher *Re* for a higher *We*. For an increasing liquid flow rate, the J-JS and JS-S transitions occurred at a lower *Re* for an increasing *We*. These trends might be explained as follows: The countercurrent air flow does two important things to the liquid flow:

(1) it introduces unsteadiness, due to pressure fluctuations associated with the gas flow; (2) due to shear at the liquid/gas interface, it thickens the liquid layer, jets, and sheets. In general, the flow unsteadiness tends to cause the break up of jets to droplets and sheets to jets at lower *Re*; however, for the J-JS and JS-S transitions, which require the creation of an intact sheet (or partial sheet), the thickening of the liquid layer by shear can be more important than the unsteadiness introduced by pressure fluctuations. The effect of shear seems more pronounced for the lower *Ga* fluid, which by comparing Figs 6 and 8 can be seen to be generally less affected by the unsteadiness introduced by the gas flow. Thus, for the lower *Ga* fluid, the J-JS and JS-S transitions occur at a lower *Re* as *We* increases. At this point, our explanation involves some conjecture and more data are needed to completely clarify the physical processes. In Fig. 8, a distinct reduction in hysteresis can also be observed with an increasing *We*. Wei and Jacobi (2002) observed this behavior in their more limited data and attributed it to unsteadiness. Some of the behavior reported now could not be observed by Wei and Jacobi (2002), because they had data at only one *Ga* and were limited to *We*<13.

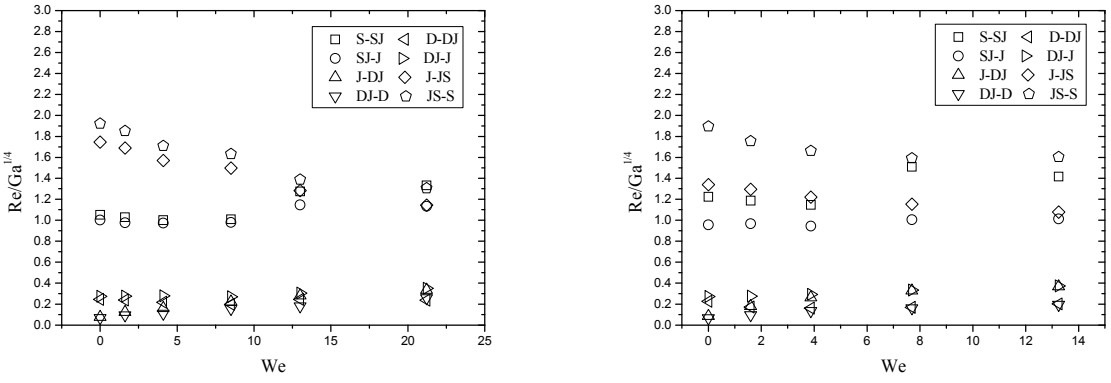

(a) (b)

Figure 8: Vapor-shear effects on falling-film mode transitions at different liquid feeding lengths, (a) L=0.1m, (b) L=0.295m, $Ga^{1/4}$≈17 (Ethylene Glycol), s/d=0.95, s/a=11.4.

4. CONCLUSIONS

New data on vapor-shear and feeding-length effects on falling-film mode transitions between horizontal tubes have been reported using two different fluids: water and ethylene glycol. A summary of the results follows:

- A simpler mode classification scheme (simpler than that of prior work) is developed and shown to be suitable for both steady and unsteady falling-film flows.
- Experiments show that the liquid feeding length has an impact on falling-film mode transitions in quiescent surroundings. For a lower *Ga* fluid, with an increasing liquid feeding length, transitions from jet mode to jet-sheet mode required a lower *Re*, which was opposite to other transitions and is probably due to edge effects.
- With an increasing *We*, the falling liquid flow became more unsteady, and when the vapor velocity was larger than about 3.5m/s, stable, steady modes were not usually present.
- Vapor shear effects on falling-film mode transitions depend on *Ga*. For a higher *Ga* fluid, the unsteady effect might be more important than the shear effect. Thus, transitions from jets to sheets occur at a higher *Re*; for a lower *Ga* fluid, the shear effect appears to be dominant with an increasing *We*. Hence, transitions between jet mode and sheet mode occur at a lower *Re*.
- A reduced hysteresis was observed when increasing *We* during experiments with a countercurrent gas flow.
- In the limited range of these experiments, transitional Reynolds numbers showed no dependence on s/d when a countercurrent gas flow was imposed.

NOMENCLATURE

a	capillary constant, $(\sigma/\rho g)^{1/2}$, (m)
d	tube diameter (m)
s	tube spacing (m)
g	gravitational acceleration (m/s^2)
L	liquid feeding length (m)
U_g	free-stream velocity of gas (m/s)
Ga	modified Galileo number, $\rho\sigma^3/\mu^4 g$
Re	Reynolds number, $2\Gamma/\mu$
We	Weber number, $\rho_g U_g^2 d/\sigma$

Greek Letter

Γ	total mass flow rate per tube length (kg/s·m)
μ	liquid dynamic viscosity (N·s/m^2)
ρ	liquid density (kg/m^3)
σ	surface tension (N/m)

Subscript

g gas

Properties with no subscript are for liquids.

REFERENCES

Armbruster, R., Mitrovic, J., 1994, Patterns of falling film flow over horizontal smooth tubes, *Pro. 10th Int. Heat Transfer Conf.,* Brighton, UK, vol. 3: p. 275-280.

Hu, X., Jacobi, A.M., 1996, The Intertube Falling Film: Part 1, Flow Characteristics, Mode Transitions and Hysteresis, *J. Heat Transfer*, vol.118, no.3: p. 616-625.

Hu, X., Jacobi, A.M., 1996, The Intertube Falling Film: Part 2, Mode Effects on Sensible Heat Transfer to a Falling Liquid Film, *J. Heat Transfer*, vol.118, no.3: p. 626-633.

Mitrovic, J., 1986, Influence of Tube Spacing and Flow Rate on Heat Transfer from a Horizontal Tube to a Falling Liquid Film, *Proc. 8th Int. Heat Transfer Conf.*, San Francisco, vol.4: p. 1949-1956.

Mitrovic, J., 2005, Flow Structures of a Liquid Film Falling on Horizontal Tubes, *Chem. Eng. Technol.* vol. 28, no.6: p. 684-694.

Ribatski,G., Jacobi, A.M., 2005, Falling-film evaporation on horizontal tubes-a critical review, *Int. J.Refrig.*, vol. 28, no. 5: p.635-653.

Roques, J. F., Dupont, V., Thome, J.R., 2002, Falling Film Transitions on Plain and Enhanced Tubes, *J. Heat Transfer*, vol.124, no.3: p. 491-499.

Roques, J.F., Thome, J.R., 2003, Falling Film Transitions Between Droplet, Column, and Sheet Flow Modes on a Vertical Array of Horizontal 19 FPI and 40 FPI Low-Finned Tubes, *Heat Transfer Eng.*, vol. 24, no.6: p.40-45.

Thome, J. R., 1999, Falling Film Evaporation: State of the Art Review of Recent Work, *J. Enhanced Heat Transfer*, vol.6, no.2-4: p.263-277.

Wei, Y. H., Jacobi, A.M., 2002, Vapor shear, geometric and bundle-depth effects on the Intertube falling-film modes, *1st Int. Conf. Heat Transfer, Fluid Mechanics, and Thermodynamics*, Kruger Park, South Africa, vol.1, no.1: p.40-60.